IOPscience iopscience.iop.org

Home Search Collections Journals About Contact us My IOPscience

Optically pumped rolled-up InAs/InGaAsP quantum dash lasers at room temperature

This content has been downloaded from IOPscience. Please scroll down to see the full text.

2013 Semicond. Sci. Technol. 28 094007

(http://iopscience.iop.org/0268-1242/28/9/094007)

View the table of contents for this issue, or go to the journal homepage for more

Download details:

IP Address: 128.97.245.130
This content was downloaded on 03/02/2014 at 14:38

Please note that terms and conditions apply.

IOP PUBLISHING SEMICONDUCTOR SCIENCE AND TECHNOLOGY
Semicond. Sci. Technol. **28** (2013) 094007 (5pp) doi:10.1088/0268-1242/28/9/094007

INVITED PAPER

Optically pumped rolled-up InAs/InGaAsP quantum dash lasers at room temperature

M H T Dastjerdi[1], M Djavid[1], S Arafin[1], X Liu[1], P Bianucci[1], Z Mi[1] and P J Poole[2]

[1] Department of Electrical and Computer Engineering, McGill University, 3480 University Street, Montreal, Quebec H3A 0E9, Canada
[2] Institute for Microstructural Sciences, National Research Council, Ottawa, Ontario K1A 0R6, Canada

E-mail: zetian.mi@mcgill.ca

Received 9 April 2013, in final form 18 June 2013
Published 21 August 2013
Online at stacks.iop.org/SST/28/094007

Abstract
We have investigated the fabrication and optical performance of free-standing rolled-up InGaAsP tube optical cavities, wherein self-organized InAs quantum dots or dashes are incorporated as the gain media. Such tubular optical cavities are formed when the coherently strained InAs/InGaAsP quantum dot/dash nanomembrane is selectively released from the host substrate. We have achieved lasing from rolled-up InAs/InGaAsP quantum dash microtubes at room temperature under continuous wave optical pumping. The measured threshold is ∼6 μW, and the Purcell factor and the spontaneous emission coupling factor are estimated to be ∼6.54 and ∼0.87, respectively.

(Some figures may appear in colour only in the online journal)

1. Introduction

The device energy budget is expected to reach ∼2–10 fJ/bit for on-chip interconnects by 2022, which is significantly smaller than that of conventional semiconductor lasers (∼300 fJ/bit, or higher) [1, 2]. Moreover, due to the large dimensions of conventional lasers as well as the materials incompatibility with Si, the achievement of highly reliable and densely integrated lasers on a CMOS chip has not been possible. Drastically different laser technologies are therefore urgently required. In this regard, low threshold, ultrahigh speed micro- and nanoscale lasers that can be directly integrated with optoelectronic and electronic components on a CMOS chip are in demand for future chip-level optical communications. Among the various semiconductor micro- and nanoscale optical cavities that have been investigated, rolled-up semiconductor tube cavities exhibit many distinct characteristics, including directional emission, controlled polarization, and ultrahigh Q-factors [3–9]. Such optical tube cavities are formed when strained nanomembranes are selectively released from the host substrate. They can be readily transferred to Si or other foreign substrates and have therefore emerged as a highly promising approach to realize high performance lasers on Si [6, 10, 11]. In addition, the three-dimensionally confined optical modes can be precisely tailored by varying the tube diameter, wall thickness, and surface geometry using standard photolithography process [12, 13].

In order to achieve ultralow threshold nanoscale lasers, self-organized quantum dots and quantum wells have been incorporated in such tubular cavities as the gain media, [7, 14–17] with lasing under optical pumping being demonstrated at room temperature [7, 18] and 4 K [16], respectively. Moreover, the direct integration of such tube devices with Si waveguides on a Si platform has been realized [8]. More recently, the fabrication and optical performance of InAs/InGaAsP quantum dot tube devices, with emission wavelengths at ∼1.5 μm, have been investigated [14]. To date, however,room temperature lasing in this wavelength range has not been reported.

 © 2013 IOP Publishing Ltd Printed in the UK & the USA

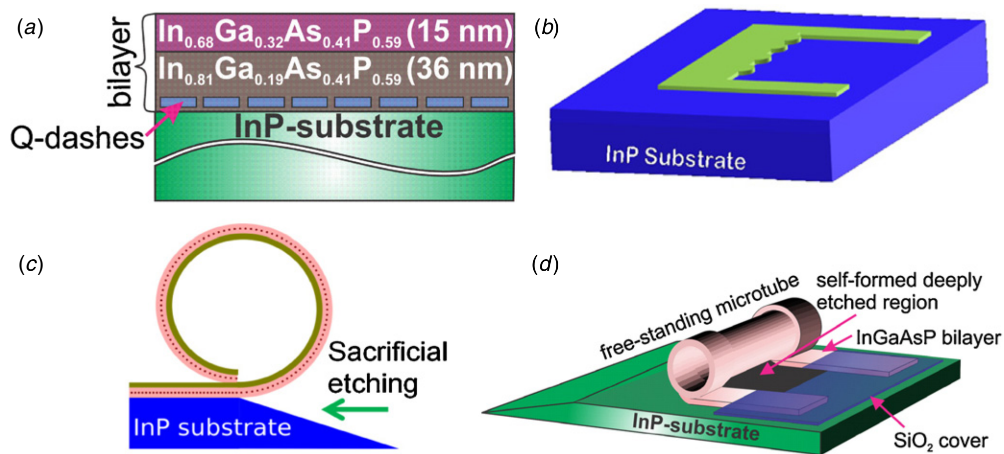

Figure 1. (*a*) Schematic illustration of InAs/InGaAsP quantum dash heterostructures grown on InP substrate. (*b*) Illustration of the U-shaped mesa. (*c*) Illustration of the formation of rolled-up InAs/InGaAsP quantum dot/dash microtubes when the underlying InP substrate is selectively etched. (*d*) Schematic of free-standing microtubes with SiO_2 protective layer covering the side pieces of the U-shaped mesa.

In this context, we have investigated the design, fabrication, and optical characteristics of free-standing InP/InGaAsP rolled-up tube optical cavities, wherein self-organized InAs quantum dot or dash heterostructures are incorporated as the gain media. The strong carrier confinement offered by the dots/dashes can drastically reduce nonradiative surface recombination in such nanomembrane devices. We have demonstrated that strong coherent emission at ~1.55 μm can be achieved in both single- and multi-turn tube optical cavities at room temperature. We have further achieved lasing at ~1.59 μm from rolled-up InAs/InGaAsP quantum dash microtubes at room temperature under continuous wave optical pumping. The measured lasing threshold is ~6 μW. The Purcell factor and the spontaneous emission coupling factor are estimated to be ~6.54 and ~0.87, respectively.

2. Experimental details

The quantum dot/dash tube device heterostructures were grown on InP substrate by chemical beam epitaxy. Schematically shown in figure 1(*a*), the coherently strained InGaAsP bilayers consist of ~36 nm $In_{0.81}Ga_{0.19}As_{0.41}P_{0.59}$ and ~15 nm $In_{0.68}Ga_{0.32}As_{0.41}P_{0.59}$, which are lattice matched to the InP substrate and tensile-strained, respectively. Such coherently strained bilayer nanomembrane, when selectively released from the host substrate, will roll into tubular structures, due to the minimization of strain. The rolling, depending on the mesa shape, generally takes place along ⟨1 0 0⟩ crystal directions [19]. The tube diameters are largely determined by the compositions and thicknesses of the InGaAsP bilayers. Two layers of self-organized InAs quantum dots/dashes are incorporated in the $In_{0.81}Ga_{0.19}As_{0.41}P_{0.59}$ layer, shown in figure 1(*a*). Detailed growth conditions for the InAs quantum dot/dash heterostructures are described elsewhere [14, 20].

Free-standing rolled-up InAs/InGaAsP quantum dot/dash tube optical cavities are fabricated using standard photolithography and wet etching techniques. A U-shaped mesa, shown in figure 1(*b*), was first defined by etching to the $In_{0.81}Ga_{0.19}As_{0.41}P_{0.59}$ layer using HCl:HNO_3:H_2O (1:2:10). The positioning of the mesas is designed such that the rolling direction of the tubes takes place along the [1 0 0] crystal direction. With selective etching of the underlying InP substrate using HCl: H_2O (2:1), the coherently strained InAs/InGaAsP quantum dot/dash heterostructures can roll into micro- or nanotubes, shown in figure 1(*c*). The central part of the resulting tube cavity will be separated from the substrate, thereby reducing any optical loss through the substrate. To ensure that the rolling process initiates only at the starting edge of the U-shaped mesa, we have previously introduced a photoresist layer to cover part of the side pieces of the U-shaped mesa [14]. In this study, we have further improved the device fabrication process by introducing a recessed SiO_2 protective layer on the two side pieces of the U-shaped mesa, shown in figure 1(*d*). The tube rolling process stops when hitting the SiO_x layer. The recessed region of the SiO_x layer between the two side pieces can ensure that the center part of the tube cavity is not in contact with SiO_2, thereby leading to reduced optical loss and high *Q*-factors. The scanning electron microscopy (SEM) image of the fabricated device is shown in figure 2(*a*), wherein the various regions are identified. Significantly, near-perfect yield can be achieved using this device fabrication process. The optical image of arrays of rolled-up InAs/InGaAsP tubes is shown in figure 2(*b*).

Additionally, the surface geometry of the rolled-up tube optical cavity can be precisely defined by introducing corrugations along the inner edge of the mesa (see figure 1(*b*)). The resulting engineered surface geometry, shown in figure 2(*c*), can provide an effective optical confinement along the tube axial direction and offer an additional dimension for controlling the optical performance of rolled-up tube lasers. In this study, the wall thickness is ~50 nm for a single-turn tube. The tube wall thickness can be further varied by controlling the number of turns, i.e. the width of the center part of the U-shaped mesa. InAs/InGaAsP quantum dot/dash tubes, with diameters in the range of ~5 to 7 μm and wall thicknesses of ~50 to 200 nm, depending on the number of turns, have been fabricated and characterized. The

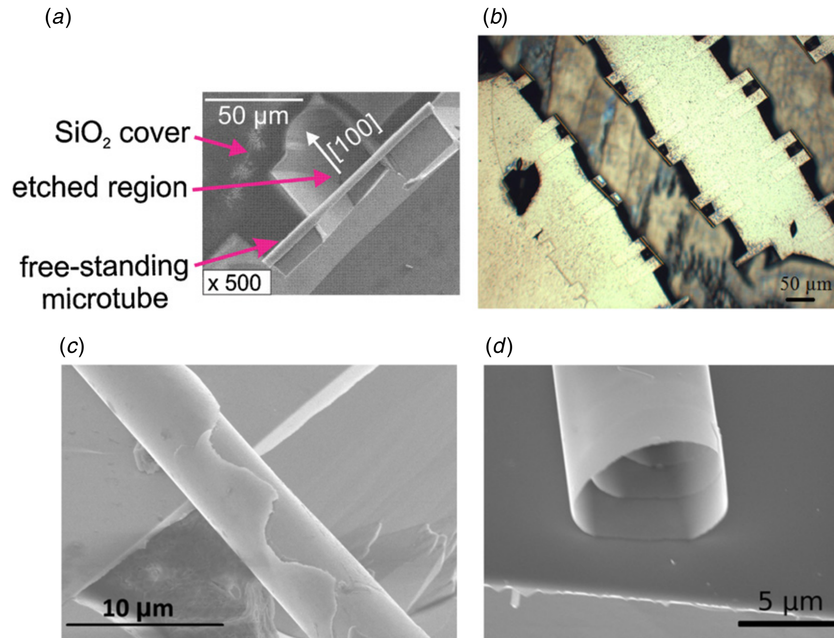

Figure 2. (*a*) SEM image of a free-standing microtube rolled along the [1 0 0] crystal direction. (*b*) Optical microscopy image from arrays of rolled-up InAs/InGaAsP tubes showing high fabrication yield. (*c*) SEM image of a microtube illustrating the engineered surface corrugations for axial mode confinement. (*d*) Cross-sectional SEM image of the microtube showing multiple turns.

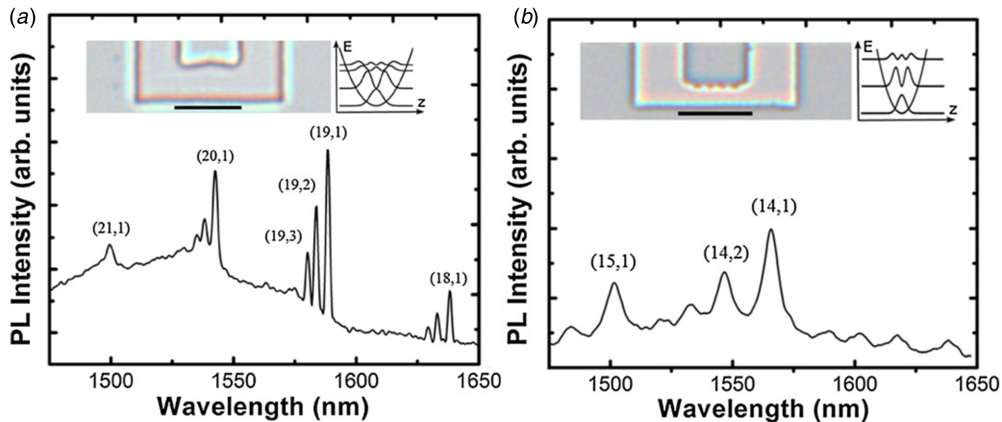

Figure 3. (*a*) Photoluminescence spectrum of a microtube with an average wall thickness of ∼100 nm. The corresponding mode numbers are identified. (*b*) Photoluminescence spectrum of a microtube with a wall thickness of ∼50 nm shown with the corresponding mode numbers. Shown in the insets are optical microscopy images of the lithographically defined U-shaped mesas, together with a schematic sketch of the electric field distribution of the first several axial modes (where the vertical separation between traces illustrates the energy separation between the modes). The scale bar corresponds to a length of 50 μm in both (*a*) and (*b*).

cross-sectional SEM image of a multi-turn tube is shown in figure 2(*d*).

A micro-photoluminescence system was used to study the optical performance of rolled-up quantum dot/dash microtube devices. The device was excited by a 635 nm laser diode through a 100× microscope objective. The emission from the sample was then collected using the same objective, directed to a high-resolution spectrometer, and detected by a liquid nitrogen-cooled InGaAs photodetector with lock-in amplification.

3. Results and discussions

Room-temperature emission characteristics of rolled-up InAs/InGaAsP quantum dot tube optical cavities are first studied. Shown in figures 3(*a*) and (*b*) are the spectra measured for a two-turn and one-turn tube, with an average wall thickness of ∼100 and 50 nm, respectively. The associated azimuthal (*m*) and axial (*p*) mode numbers are identified [12, 21]. The spacing between consecutive azimuthal modes is ∼23 meV and 34 meV, for the two-turn and one-turn tubes with diameters of ∼5 μm, respectively. The wall thickness also plays an important role in determining the mode properties. It is seen that for the two-turn tube, the linewidth is much narrower (∼0.9 meV), compared to that (∼3 meV) of the one-turn tube, due to the enhanced optical confinement associated with the increased wall thickness. We have further measured an extremely high cold-cavity *Q*-factor (∼1.5 × 10^5) for a five-turn GaAs-based tube optical cavity [8]. Such high cold-cavity

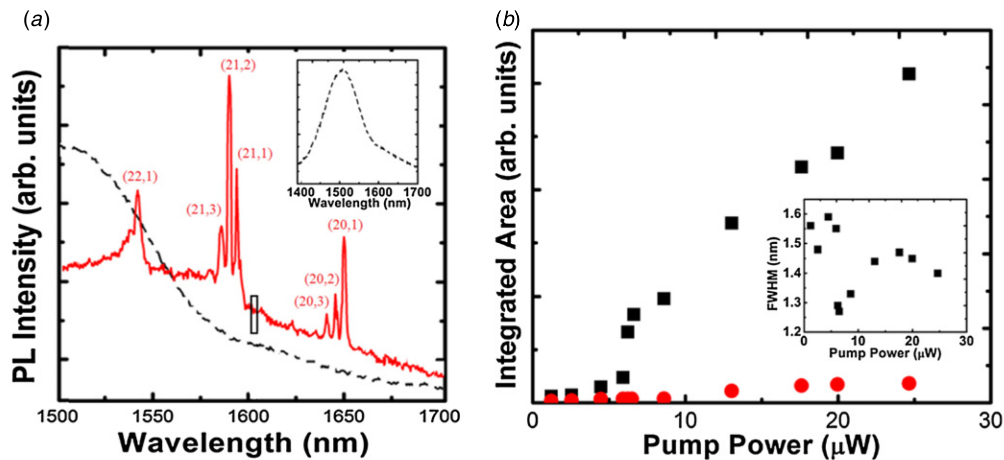

Figure 4. (*a*) Photoluminescence spectrum of a quantum dash microtube measured at room temperature with an incident pump power of ∼19.9 μW. The measured spectrum of the as-grown quantum dash sample is shown as the dashed lines and also in the inset. The curves are vertically shifted for display purpose. (*b*) Integrated intensity versus pump power for the mode (21,2) and for the background emission extracted from the box shown in (*a*). The inset shows the FWHM of the mode (21,2) measured under various incident pump powers.

Q-factor is also expected from InP-based tube devices, given that they exhibit similar geometries and dimensions.

Additionally, it is observed that the axial modes can be controlled by varying the tube surface geometry. The shapes of the inner edge of the lithographically defined mesas are shown in the left insets of figures 3(*a*) and (*b*) for the two-turn and one-turn tube cavities, respectively. Schematic electric field distributions, based on analytic models for microtube and bottle resonators, are also sketched in the right insets [21, 22]. The surface corrugations of the two-turn and one-turn devices exhibit correspondingly low and high curvatures. The resulting weak and strong axial optical confinements yield relatively small (∼2.3 meV) and large (∼9.5 meV) energy spacing between adjacent axial modes for the two-turn and one-turn tube devices, respectively. It is therefore evident that the three-dimensionally confined optical modes can be tailored by varying the tube diameter, wall thickness and surface geometry using a simple, high-throughput, optical lithographical step. Lasing at ∼1.47 μm has been further achieved from such quantum dot tube cavities at 82 K under optical pumping [14].

To achieve lasing at room temperature, we have studied rolled-up tube cavities with the incorporation of InAs quantum dashes, which can exhibit relatively large saturation gain. The emission spectrum measured from the tube at an excitation power of ∼19.9 μW is shown in figure 4(*a*). The corresponding azimuthal and axial mode numbers are identified. For comparison, also shown in the figure is the photoluminescence spectrum measured from the as-grown InAs quantum dash sample. The optical modes were analyzed by fitting them using Lorentzian functions to extract the corresponding integrated area and full-width-at-half-maximum (FWHM) at each excitation power level. Figure 4(*b*) shows the integrated intensity versus pump power for the mode (21,2) (at ∼1590 nm). A clear threshold is observed at ∼6 μW excitation power level. Variations of the FWHM of this mode versus pump power are shown in the inset. A reduction of the spectral linewidth from ∼1.6 to 1.25 nm is also measured at the threshold, suggesting the achievement of lasing. In this study, the measured minimum linewidth may be limited by the presence of two nearly degenerate modes, due to the spiral symmetry of the tube structure [23]. In addition, an abrupt linewidth narrowing above threshold may not be expected, given the large spontaneous emission coupling factor (described below) [24]. It may also be noticed that the linewidth showed a small increase with increasing power, due to the heating effect of the tube device [25]. To further confirm the lasing behavior, we have derived the integrated background emission at different pump powers by calculating the integrated area of a spectral width of ∼4 nm separated by ∼12 nm from the mode (21,2) (see the square box in figure 4(*a*)). It is seen that the background emission is negligibly small and stays nearly constant at or above threshold power, shown in figure 4(*b*). With further increasing pump power, the background emission is slightly enhanced, due to the hot carrier effect commonly observed in quantum dot/dash lasers [26].

Similar analysis was performed for other modes shown in figure 4(*a*). However, a clear linewidth reduction or threshold behavior in the light–light plot was not measured, indicating lasing was not achieved for these modes. The underlying reason has been investigated. It is noticed that the mode (22,1) shows weaker emission, compared to the mode (21,2), which is in direct contrast to the strong photoluminescence emission from the as-grown sample in the wavelength range of ∼1540 nm. Additionally, the mode (20,1) exhibits comparatively strong intensity in spite of the extremely weak photoluminescence emission from the as-grown sample in this wavelength range. This discrepancy is explained by the wavelength-dependent cavity *Q*-factor. Due to the large inhomogeneity of InAs quantum dashes, the cavity *Q*-factors for resonance modes at shorter wavelengths suffer severely from the photon absorption by non-resonant quantum dashes with relatively small transition energies. The reduction of the *Q*-factor of rolled-up tube optical cavities, due to the optical absorption by the quantum dots/dashes, has been further confirmed by the transmission measurements of such structures [25]. Additionally, the *Q*-factor associated with

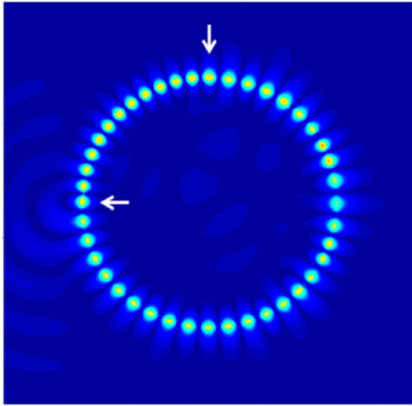

Figure 5. Simulated distribution of the resonance mode in a rolled-up InGaAsP microtube with a radius of ∼2.4 μm and wall thickness of ∼100 nm by the two-dimensional finite-difference time-domain method. The presence of inside and outside notches are shown by the arrows.

various axial modes can be strongly influenced by the shape of the surface geometry during the device fabrication process.

Compared to an ideal ring resonator, the Q-factor of rolled-up tube cavities is further limited by the rapid change in thicknesses at the discontinuous rolling edges, i.e. the inside and outside notches, which leads to strong light scattering. Illustrated in figure 5 is the distribution of the simulated optical resonance mode (azimuthal mode of 21) for a microtube with a wall thickness of ∼100 nm by the two-dimensional finite-difference time-domain method. It is seen that light scattered out by the inside notch can serve as useful output from rolled-up tube lasers, thereby leading to micro/nanoscale lasers with controlled directional emission. Moreover, the output coupling efficiency can be varied by controlling the number of turns. For example, a larger Q-factor can be achieved in rolled-up tube cavities with multi-turns, compared to a single-turn device.

The maximum Purcell factor is further estimated for the combined quantum dash/microcavity system using the following formula [27],

$$F_P = \frac{3}{4\pi^2}\left(\frac{\lambda_c}{n_{\rm eff}}\right)^3 \frac{Q}{V_{\rm eff}} \qquad (1)$$

where λ_c is the resonance wavelength, $V_{\rm eff}$ is the effective mode volume, and $n_{\rm eff}$ is the effective refractive index. For the lasing mode (21,2), Q is ∼1,200, and $V_{\rm eff}$ and $n_{\rm eff}$ are estimated to be ∼8 μm^3 and ∼1.91, respectively [28]. The Purcell factor is derived to be ∼6.54. The spontaneous emission coupling factor (β) is further estimated to be ∼0.87, indicating strong coupling of the spontaneous emission to the cavity mode.

4. Conclusion

In summary, we have performed a detailed investigation of the design, epitaxial growth, fabrication, and characterization of rolled-up InAs quantum dot/dash tube optical cavities. Such devices can be readily transferred on Si substrates for integrated nanophotonic circuits on a Si-platform. Moreover, with the use of quantum dot/dash gain media and by engineering the diameter, wall thickness and surface geometry of the tube cavities, both single- and multi-wavelength micro- and nanoscale lasers can be realized, which promise a host of new functionalities, including the realization of chip-level dense wavelength-division multiplexing systems on Si.

Acknowledgments

This work was supported by US Army Research Office under the grant W911NF-12-1-0477 and the Natural Sciences and Engineering Research Council of Canada (NSERC). The device fabrication work was performed in the McGill University Nanotools Microfab facility.

References

[1] Miller D A B 2009 *Proc. IEEE* **97** 1166
[2] Miller D A B 2010 *Appl. Opt.* **49** F59
[3] Prinz V Y, Seleznev V A, Gutakovsky A K, Chehovskiy A V, Preobrazhensky V, Putyato M A and Gavrilova T A 2000 *Physica* E **6** 828
[4] Kipp T, Welsch H, Strelow C, Heyn C and Heitmann D 2006 *Phys. Rev. Lett.* **96** 077403
[5] Schmidt O G and Eberl K 2001 *Nature* **410** 168
[6] Vicknesh S, Li F and Mi Z 2009 *Appl. Phys. Lett.* **94** 081101
[7] Li F and Mi Z 2009 *Opt. Express* **17** 19933
[8] Tian Z B, Veerasubramanian V, Bianucci P, Mukherjee S, Mi Z, Kirk A G and Plant D V 2011 *Opt. Express* **19** 12164
[9] Mi Z and Bianucci P 2012 *Curr. Opin. Solid. State Mater. Sci.* **16** 52
[10] Tian Z B, Li F, Mi Z and Plant D V 2010 *IEEE Photon. Technol. Lett.* **22** 311
[11] Chun I and Li X 2008 *IEEE Trans. Nanotechnol.* **7** 493
[12] Li F, Mi Z and Vicknesh S 2009 *Opt. Lett.* **34** 2915
[13] Strelow C, Rehberg H, Schultz C, Welsch H, Heyn C, Heitmann D and Kipp T 2008 *Phys. Rev. Lett.* **101** 127403
[14] Bianucci P, Mukherjee S, Dastjerdi M H T, Poole P J and Mi Z 2012 *Appl. Phys. Lett.* **101** 031104
[15] Chun I S, Bassett K, Challa A and Li X L 2010 *Appl. Phys. Lett.* **96** 251106
[16] Strelow C, Sauer M, Fehringer S, Korn T, Schuller C, Stemmann A, Heyn C, Heitmann D and Kipp T 2009 *Appl. Phys. Lett.* **95** 221115
[17] Mendach S, Songmuang R, Kiravittaya S, Rastelli A, Benyoucef M and Schmidt O 2006 *Appl. Phys. Lett.* **88** 111120
[18] Heo J, Bhowmick S and Bhattacharya P 2012 *IEEE J. Quantum Electron.* **48** 927
[19] Chun I S, Challa A, Derickson B, Hsia K J and Li X L 2010 *Nano Lett.* **10** 3927
[20] Poole P J, Kaminska K, Barrios P, Lu Z and Liu J 2009 *J. Cryst. Growth* **311** 1482
[21] Strelow C, Schultz C, Rehberg H, Welsch H, Heyn C, Heitmann D and Kipp T 2007 *Phys. Rev.* B **76** 045303
[22] Louyer Y, Meschede D and Rauschenbeutel A 2005 *Phys. Rev.* A **72** 031801
[23] Hosoda M and Shigaki T 2007 *Appl. Phys. Lett.* **90** 181107
[24] Bjork G and Yamamoto Y 1991 *IEEE J. Quantum Electron.* **27** 2386
[25] Tian Z B, Bianucci P, Roche P J R, Dastjerdi M H T, Mi Z, Poole P J, Kirk A G and Plant D V 2012 *Opt. Lett.* **37** 2712
[26] Bhattacharya P and Mi Z 2007 *Proc. IEEE* **95** 1723
[27] Purcell E M 1946 *Phys. Rev.* **69** 681
[28] Srinivasan K, Borselli M and Painter O 2006 *Opt. Express* **14** 1094